

## Hydrogen-Bond-Based Magnetic Exchange Between $\mu$ -Diethylnicotinamide(aqua)bis(X-salicylato)copper(II) Polymeric Chains

Maria Korabik,\*<sup>[a]</sup> Zuzana Repická,<sup>[b]</sup> Ladislav Martiška,<sup>[b]</sup> Jan Moncol,<sup>[b]</sup> Jozef Švorec,<sup>[b]</sup> Zdeňka Padělková,<sup>[c]</sup> Tadeusz Lis,<sup>[a]</sup> Milan Mazúr,<sup>[d]</sup> and Dušan Valigura\*<sup>[b]</sup>

*In Memory of Professor Tadeusz Głowiąk*

**Keywords:** Coordination polymer; Copper; Hydrogen bonds; Magnetic properties; Supramolecular chemistry

**Abstract.** Polymeric salicylatocopper(II) complexes of unusual composition  $[\text{Cu}(\text{X-sal})_2(\mu\text{-denia})(\text{H}_2\text{O})]_n$  [denia = diethylnicotinamide, and X-sal = 5-methylsalicylate (**1**), 3-methylsalicylate (**2**), 4-methoxysalicylate (**3**), 3,5-dichlorosalicylate (**4**) and 3,5-dibromosalicylate (**5**)] were synthesized and characterized. Magnetic measurements were performed in the temperature range 1.8–300 K. The structural unit of all complexes consists of a Cu<sup>II</sup> atom, which is monodentately coordinated by the pair of X-salicylate anions in *trans* positions. Water and the diethylnicotinamide ligand occupy the other two basal plane positions of the tetragonal pyramid. The axial positions are occupied by a diethylnicotinamide oxygen atom of neighboring structural units, thus forming a spiral polymeric structure parallel to *b* axis. Magnetic measure-

ments showed that all complexes **1–5** exhibit a susceptibility maximum at about 6–8 K. The obtained data fit to Bleaney–Bowers equation gave singlet-triplet energy gaps  $2J = -8.60 \text{ cm}^{-1}$  for **1**,  $2J = -6.57 \text{ cm}^{-1}$  for **2**,  $2J = -8.57 \text{ cm}^{-1}$  for **3**,  $2J = -6.82 \text{ cm}^{-1}$  for **4**, and  $2J = -6.45 \text{ cm}^{-1}$  for **5**. The supramolecular structure based on hydrogen bonds [described by supramolecular synthons  $R_2^2(10)$  and  $R_2^2(12)$ ] is the pathway for antiferromagnetic interactions of the magnetically coupled pairs of copper atoms of neighboring chains within the 2D supramolecular layers. The results of the magnetic measurements suggest involvement of the COO groups in the magnetic interaction pathway for all five complexes.

### Introduction

It is no surprise, that hydrogen bonds play an important role in various fields of science from biology to technical applications, including coordination chemistry.<sup>[1]</sup> In the solid state, hydrogen bonds mainly effect the mutual positions of molecules and allow the formation of different 1D, 2D, or 3D supramolecular structures.<sup>[2]</sup> Complexes linked by hydrogen bonds

are more stable but have a higher flexibility. They exhibit a fascinating structural diversity and have potential applications<sup>[3]</sup> in catalysis,<sup>[4]</sup> the synthesis of chiral structures, luminescence,<sup>[5]</sup> magnetism,<sup>[6]</sup> nonlinear optics,<sup>[7]</sup> different sensor applications, drug design, and porosity exploitation in separation techniques.<sup>[8]</sup> The unusual dimeric complex  $[\text{Cu}(5\text{-MeOsal})_2(\mu\text{-nia})(\text{H}_2\text{O})]_2$  (5-MeOsal = 5-methoxysalicylate anion, nia = nicotinamide)<sup>[9]</sup> exhibits interesting properties, including magnetic interactions mediated by hydrogen bonds. Its antiferromagnetic properties, which were characterized by the singlet-triplet energy gap ( $2J = -6.83 \text{ cm}^{-1}$ ) were attributed to interdimer Cu $\cdots$ Cu interactions through carboxylate bridges extended by O–H $\cdots$ O hydrogen bonds. Recently, a monomeric nitrobenzoatocopper(II)  $[\text{Cu}(3\text{-O}_2\text{Nbz})_2(\text{nia})(\text{H}_2\text{O})_2]$  complex with similar magnetic behavior has been published and its monomeric molecular structure with supramolecular dimer formation<sup>[10]</sup> has proved the previously suggested pathway<sup>[9]</sup> of antiferromagnetic interaction and has given the base for understanding that the spin–spin interaction and consequently the form of magnetic dimensionality could be different from its structural dimensionality.

In this report, we describe the synthesis, structure, spectral, and magnetic properties of five salicylatocopper(II) coordination polymers:  $[\text{Cu}(5\text{-Mesal})_2(\mu\text{-denia})(\text{H}_2\text{O})]_n$  (**1**),  $[\text{Cu}(3\text{-Mesal})_2(\mu\text{-denia})(\text{H}_2\text{O})]_n$  (**2**),  $[\text{Cu}(4\text{-MeOsal})_2(\mu\text{-denia})(\text{H}_2\text{O})]_n$  (**3**),  $[\text{Cu}(3,5\text{-Cl}_2\text{sal})_2(\mu\text{-denia})(\text{H}_2\text{O})]_n$  (**4**), and  $[\text{Cu}(3,5\text{-$

\* Dr. M. Korabik  
E-Mail: jkorab@wchuwr.chem.uni.wroc.pl  
\* Prof. Dr. D. Valigura  
E-Mail: dusan.valigura@stuba.sk

[a] Faculty of Chemistry  
University of Wrocław  
14 Joliot-Curie St.  
50-383 Wrocław, Poland

[b] Department of Inorganic Chemistry  
Slovak University of Technology  
Radlinského 9  
812 37 Bratislava, Slovakia

[c] Department of General and Inorganic Chemistry  
Faculty of Chemical Technology, University of Pardubice  
Nám. Čs. Legií 565  
53210 Pardubice, Czech Republic

[d] Department of Physical Chemistry  
Slovak University of Technology  
Radlinského 9  
812 37 Bratislava, Slovakia

Supporting information for this article is available on the WWW under <http://dx.doi.org/10.1002/zaac.201000301> or from the author.

$\text{Br}_2\text{sal})_2(\mu\text{-denia})(\text{H}_2\text{O})_n$  (**5**) (5-Mesal = 5-methylsalicylate; 4-MeOsal = 4-methoxysalicylate; 3,5-Cl<sub>2</sub>sal = 3,5-dichlorosalicylate, 3,5-Br<sub>2</sub>sal = 3,5-dibromosalicylate, denia = diethylnicotinamide), which have a similar magnetic susceptibility versus temperature behavior due to their similar structures.

## Results and Discussion

### Structure of $[\text{Cu}(\text{X-sal})_2(\mu\text{-denia})(\text{H}_2\text{O})_n$ (**1–5**)

The structures of compounds **1–5** contain one-dimensional chains parallel to the *b* axis. The independent part of each chain is, in all five cases, formed by a copper(II) atom coordinated in square pyramidal manner. The basal plane of each Cu<sup>II</sup> coordination polyhedron is formed by two carboxylato oxygen atoms (O12 and O13) of two salicylato ions in *trans* positions (Figure 1).

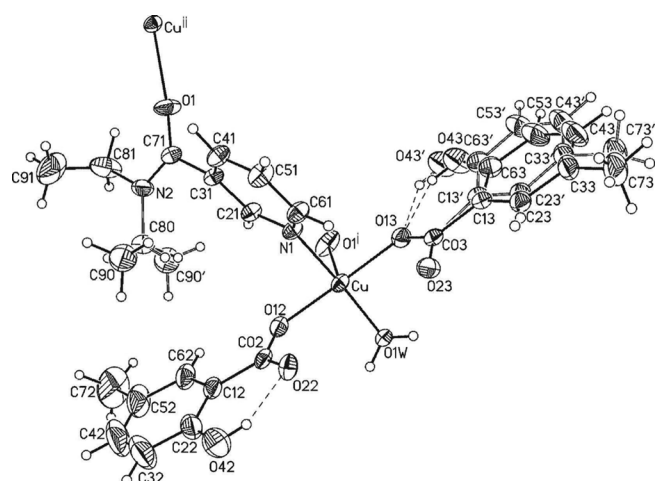


**Figure 1.** View of  $[\text{Cu}(5\text{-Mesal})_2(\mu\text{-denia})(\text{H}_2\text{O})_n$ ] (**1**), with the atom numbering scheme. Thermal ellipsoids are drawn at the 30 % probability level. [Symmetry code: (i)  $-x-1/2, y-1/2, -z+3/2$ ; (ii)  $-x-1/2, y+1/2, -z+3/2$ ].

The pyridine nitrogen atom N1 of denia ligand and the oxygen atom of the water molecule O1W are occupying the remaining two basal plane positions. The apical position of each square pyramid is occupied by the carboxamide oxygen atom O1 of the adjacent symmetry-related denia molecule, thus forming a spiral 1D chain (Figure 2). The interatomic distances and bond angles for all five complexes coordination polyhedra are shown in Table 1.

The neighboring chains are linked by the hydrogen atoms H1W and/or H2W of coordinated water molecules to the uncoordinated carboxylate oxygen atoms O13 or O23 of the adjacent polymeric chain (Figure 3). The hydrogen bonding parameters are given in Table 1. Pairs of the supramolecular synthons  $R_2^2(10)$  and  $R_2^2(12)$  formed between the adjacent copper(II) atoms (Scheme 1) are observed, which are similar to those found in complexes of lower dimensionalities,  $[\text{Cu}(5\text{-MeOsal})_2(\mu\text{-nia})(\text{H}_2\text{O})_2]$ <sup>[9]</sup> and/or  $[\text{Cu}(3\text{-O}_2\text{Nbz})_2(\text{nia})(\text{H}_2\text{O})_2]$ <sup>[10]</sup>.

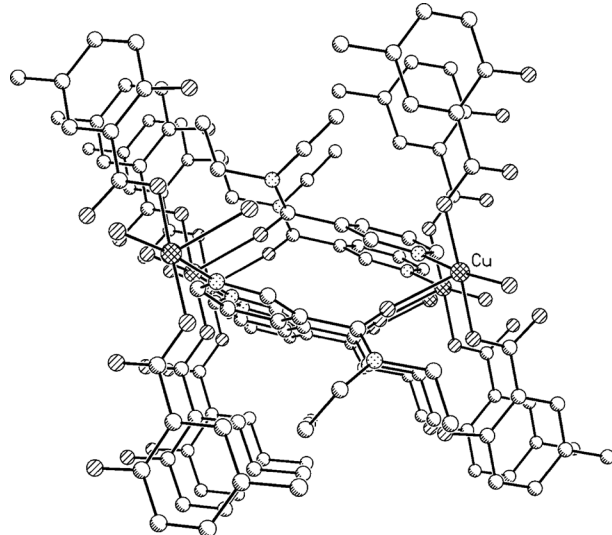


**Figure 2.** Perspective view of  $[\text{Cu}(5\text{-Mesal})_2(\mu\text{-denia})(\text{H}_2\text{O})_n$ ] spiral chain. The minority parts of disordered groups and the hydrogen atoms are omitted for clarity.

### Supramolecular Structure Relation to Magnetic Properties

The analogy of the hydrogen bridges was the reason for magnetic measurements of all complexes **1–5**. They exhibited similar magnetic susceptibility versus temperature functions with a maximum of the susceptibility in the range 6–8 K (Figure 4 for **1**, Figures S4–S7 for **2–5**, Supporting Information, and Table 2 for the data of all complexes).

The dimeric complex  $[\text{Cu}(5\text{-MeOsal})_2(\mu\text{-nia})(\text{H}_2\text{O})_2]$ <sup>[9]</sup> and especially the monomeric complex  $[\text{Cu}(3\text{-O}_2\text{Nbz})_2(\text{nia})(\text{H}_2\text{O})_2]$ <sup>[10]</sup> as well as all five complexes presented in this paper exhibit similar magnetic properties, despite their different structural dimensionalities. The first presented complex (see above) is dimeric with nicotinamide bridges,<sup>[9]</sup> but the second is a monomer without any bridging molecules except the mentioned hydrogen bonds, so no other pathway than the system of hydrogen bonds including carboxylate groups and water molecules coordinated to neighboring copper(II) atoms, described by supramolecular synthons  $R_2^2(10)$  and  $R_2^2(12)$  (Scheme 1), is possible.

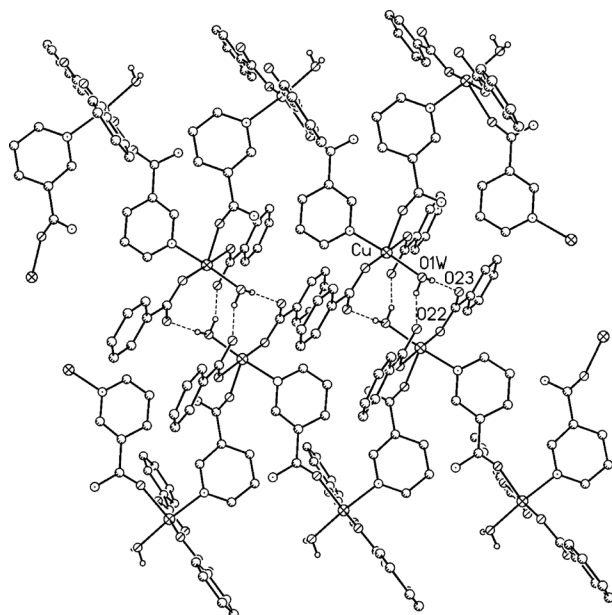
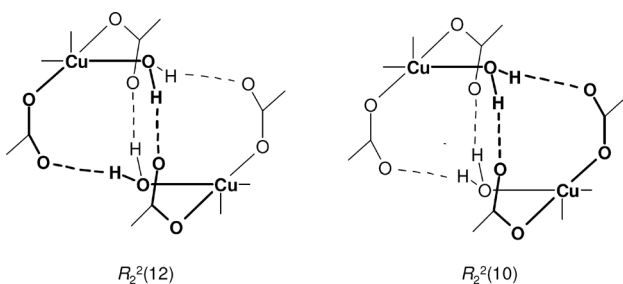
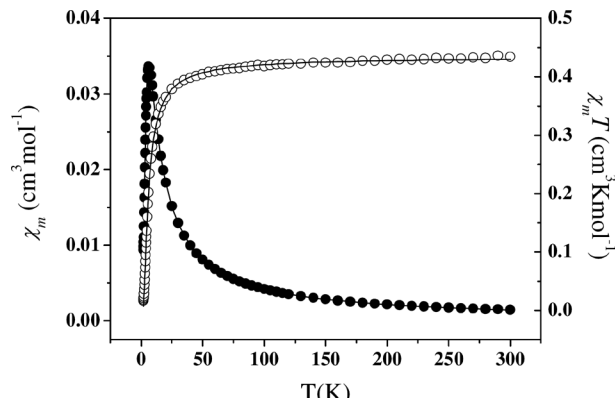
The strong hydrogen bonding interactions connect the closest copper(II) ions and are the base of the pathway for the antiferromagnetic exchange interactions. To estimate the magnitude of the coupling, the Bleaney–Bowers<sup>[11]</sup> susceptibility equation, derived from spin Hamiltonian  $H = -2JS_1S_2$ , was used for evaluation:

$$\chi_m = \frac{N\beta^2 g^2}{3kT} \left[ 1 + \frac{1}{3} \exp\left(\frac{-2J}{kT}\right) \right]^{-1}$$

Taking into consideration the expanded structures of polymeric complexes **1–5**, the molecular field model<sup>[12]</sup> was added to describe other interactions:

**Table 1.** Selected bond lengths and hydrogen bond parameters /Å, ° for **1–5**.

	<b>1</b>	<b>2</b>	<b>3</b>	<b>4</b>	<b>5</b>
Cu–O12	1.949(2)	1.935(2)	1.972(2)	1.962(2)	1.958(4)
Cu–O13	1.943(2)	1.938(2)	1.943(2)	1.956(2)	1.951(4)
Cu–N1	2.007(2)	2.010(2)	2.013(2)	2.006(3)	2.008(5)
Cu–O1W	1.954(2)	1.955(2)	1.957(2)	1.962(2)	1.957(3)
Cu–O1 <sup>i</sup>	2.368(2)	2.351(2)	2.386(2)	2.316(3)	2.311(4)
O12–Cu–O13	178.0(1)	176.5(1)	176.7(1)	177.3(1)	177.4(2)
N1–Cu–O1W	173.0(1)	168.9(1)	172.2(1)	176.8(1)	175.6(2)
O1–Cu–O12	90.3(1)	87.7(1)	87.8(1)	91.8(1)	92.2(2)
O1–Cu–N1	92.2(1)	94.0(1)	91.6(1)	88.4(1)	89.5(2)
O1–Cu–O13	87.7(1)	88.8(1)	88.9(1)	90.6(1)	90.2(2)
O1–Cu–O1W	94.5(1)	97.1(1)	96.1(1)	94.8(1)	94.7(2)
H1W…O22	1.88	1.81	1.86	1.81	1.81
O1W…O22	2.671(3)	2.645(3)	2.690(3)	2.649(3)	2.649(6)
O1W–H1W…O22	160	170	171	172	173
H2W…O23	1.83	1.87	1.82	1.82	1.83
O1W…O23	2.643(3)	2.706(3)	2.651(2)	2.651(3)	2.648(5)
O1W–H2W…O23	166	172	170	168	166

Symmetry code: (i)  $-x-1/2, y-1/2, -z+3/2$ .**Figure 3.** Perspective view of hydrogen bonds interactions between adjacent  $[\text{Cu}(5\text{-Mesal})_2(\mu\text{-denia})(\text{H}_2\text{O})]_n$  spiral chains. The minority parts of disordered groups; ethyl, methyl, and hydroxyl groups; and the hydrogen atoms are omitted for clarity.**Scheme 1.** Supramolecular synthons formed by hydrogen bonds.**Figure 4.** Temperature dependence of  $\chi_m$  (●) and  $\chi_m T$  (○) for **1** ( $\chi_m$  being the molar magnetic susceptibility per copper ion). Solid lines were obtained for calculated parameters:  $g = 2.16 \pm 0.02$ ,  $2J = -8.60 \pm 0.03 \text{ cm}^{-1}$ ,  $zJ' = -0.8 \pm 0.1 \text{ cm}^{-1}$ ,  $R = 1.6 \times 10^{-4}$ .

$$\chi_m^{\text{corr}} = \frac{\chi_m}{1 - \frac{2zJ' \chi_m}{N\beta^2 g^2}}$$

where  $\chi_m$  is the molar susceptibility given by the Bleaney–Bowers equation,  $zJ'$  characterizes all other magnetic interactions, and  $z$  is the number of the nearest neighbors. Other symbols have their usual meaning:  $N$  is the Avogadro number,  $g$  is the spectroscopic splitting factor,  $\beta$  is the Bohr magneton, and  $k$  is the Boltzmann constant. The best fit parameters obtained are given in Table 2, together with additional structural data. The resulting singlet-triplet energy gaps  $2J$  of complexes **1–5** are in the range  $6\text{--}8 \text{ cm}^{-1}$  and are in good agreement with the temperature of magnetic susceptibility maximum (Table 2). The temperature  $T_{\max}$  is related to  $2J$  according to  $|2J| / kT_{\max} = 1.599$ ,<sup>[12]</sup> the observed values follow this relation.

The obtained best fit parameters, the singlet-triplet energy gap  $2J$  of **1** and **3** differ from the previously obtained values

**Table 2.** Magnetic measurements and structural data for magneto-structural analysis of **1–5**.

	<b>1</b>	<b>2</b>	<b>3</b>	<b>4</b>	<b>5</b>
$\mu_{\text{eff}}$ /B.M. (1.8 K)	0.23	0.33	0.13	0.37	0.38
$\mu_{\text{eff}}$ /B.M. (300 K)	1.89	1.87	1.88	1.83	1.78
$T_{\max}$ /K	8.0	6.0	8.0	6.0	6.0
$2J/\text{cm}^{-1}$	$-8.60 \pm 0.03$	$-6.57 \pm 0.01$	$-8.57 \pm 0.01$	$-6.82 \pm 0.07$	$-6.45 \pm 0.07$
$zJ'/\text{cm}^{-1}$	$-0.8 \pm 0.1$	$-0.29 \pm 0.03$	$-0.38 \pm 0.03$	$-0.94 \pm 0.08$	$-0.78 \pm 0.08$
$g$	$2.16 \pm 0.02$	$2.18 \pm 0.01$	$2.17 \pm 0.01$	$2.15 \pm 0.01$	$2.13 \pm 0.01$
$R$	$1.6 \times 10^{-4}$	$1.4 \times 10^{-4}$	$1.2 \times 10^{-5}$	$8.3 \times 10^{-5}$	$8.9 \times 10^{-5}$
$\tau$	0.083	0.126	0.074	0.008	0.030
Cu…Cu <sup>a)</sup>	4.622	4.798	4.767	4.946	4.923
Cu…Cu <sup>b)</sup>	8.311	8.386	8.475	8.284	8.249
Cu…Cu <sup>c)</sup>	8.126	8.165	8.155	8.065	8.105
Basal plane–basal plane	3.219	3.321	3.303	3.190	3.179
Cu…basal plane	0.041	0.066	0.039	0.047	0.057
O1W…O22 <sup>iii</sup>	2.671	2.645	2.689	2.649	2.648
O1W…O23 <sup>iii</sup>	2.643	2.707	2.649	2.651	2.647
O1W…Cu(COO) <sub>2</sub> plane	1.295	1.350	1.356	1.305	1.297
H1W…Cu(COO) <sub>2</sub> plane	1.019	1.026	1.010	0.981	1.027
H2W…Cu(COO) <sub>2</sub> plane	1.064	0.981	0.986	0.982	0.919

a) Cu…Cu distance of atoms connected by hydrogen bonds. b) Cu…Cu distance of atoms connected by denia bridging molecule. c) Cu…Cu distance of atoms next to each other within the spiral.

for  $[\text{Cu}(5\text{-MeOsal})_2(\mu\text{-nia})(\text{H}_2\text{O})]_2$  ( $2J = -6.83 \text{ cm}^{-1}$ )<sup>[9]</sup> or  $[\text{Cu}(3\text{-O}_2\text{Nbz})_2(\text{nia})(\text{H}_2\text{O})]_2$  ( $2J = -6.25 \text{ cm}^{-1}$ )<sup>[10]</sup> whereas the  $2J$  values of **2**, **4**, and **5** are similar to those previously obtained. It is easy to relate those two greater  $-2J$  values ( $8.60 \text{ cm}^{-1}$  for **1** and  $8.57 \text{ cm}^{-1}$  for **3**, respectively) to the two shortest (4.62 Å for **1** and 4.77 Å for **3**, respectively) Cu…Cu<sup>A</sup> distances of the copper atoms connected by hydrogen bonds. It is obvious that the Cu…Cu<sup>A</sup> distance is not the only factor influencing the interaction. An additional influence could be documented by the structure of complex **2** in which the Cu…Cu<sup>A</sup> distance is only slightly greater (4.80 Å) than in complex **3**, but the value of the  $-2J$  parameter drops significantly to  $6.57 \text{ cm}^{-1}$ .

On the other hand, complexes **1** and **3** exhibit an almost perfect square-pyramidal coordination environment, which is confirmed by  $\tau$  parameter<sup>[13]</sup> values of 0.083 and 0.074, respectively (Table 2), whereas the slightly more distorted square-pyramidal arrangement of complex **2** ( $\tau = 0.126$ ) could partly explain differences in the strength of magnetic exchange interactions ( $2J$ ) within this group of complexes. However, this conclusion cannot be simply extended to complexes **4** and **5**. Here, the distortion of the square-pyramidal arrangement that decreases the overlap of  $d_{x^2-y^2}$  magnetic orbitals<sup>[12]</sup> of copper atoms and consequently decreases the strength of magnetic exchange interactions has only little influence. Additionally, complex **2** differs from the complexes **1** or **3** by the “bent” position of both COO groups out of the plane defined by the apical oxygen atom O1, the copper atom and both oxygen atoms O12 and O13. These dihedral angles (P1–P2, and/or P1–P3) are defined to some extent similarly as the  $\varphi_{\text{bent}}$  angle<sup>[13]</sup> for the series of the “paddle-wheel” aromatic copper(II) carboxylate functions, where the “abnormally” small value of  $-2J = 267 \text{ cm}^{-1}$  (in comparison to values in the range 316–350 cm<sup>-1</sup>) was attributed to the average  $\varphi_{\text{bent}}$  angle of 11.4(3) °. In our case, the average (P1–Pi)<sub>aver</sub> values are in

fairly good agreement with the obtained  $-2J$  values from magnetic measurements (Table 3), thus confirming the idea that the carboxylato groups are involved in magnetic interaction pathway. By changing the  $\varphi_{\text{bent}}$  angle value the overlap between the  $d_{x^2-y^2}$  magnetic orbital of the Cu<sup>II</sup> atoms and the 2p oxygen orbital of the bridge decreases. The P2–P3 angle values given in Table 3 show that the COO groups are “bent” symmetrically and remain nearly coplanar for complex **3**, whereas in all other complexes additional “twisting” of the COO groups is present. It should be noted that the studied complexes slightly differ in mutual orientation of the carboxylato phenyl rings (Table 3 and Table S1). There is no simple relationship between magnetic ( $2J$ ) and structural (e.g. Cu…Cu) parameters and it is logically supported by the suggestion that the exchange pathways between interacting ions are no simple bridges. Similar conclusions were drawn by Reedijk et al.<sup>[14]</sup> They explained magnetic exchange interactions in dinuclear copper(II) units with the double [O…H(water)] bridge, resulting in antiferromagnetic interactions between the Cu<sup>II</sup> ions separated at a distance of 4.8896 Å, with a singlet-triplet energy gap of  $-19.8 \text{ cm}^{-1}$ .

The data discussed above (Table 2 and Table 3) confirm that the antiferromagnetic interaction of copper atoms with unpaired spins is realized by specific positioning of coordinated ligands originated in hydrogen bond formation similar to those previously reported.<sup>[9,10,15]</sup> A theoretical investigation of exchange coupling through hydrogen bonding<sup>[16]</sup> has given the idea, that hydrogen bonds are responsible for fixing molecules, in our cases macromolecules, in position allowing overlap of magnetic orbitals. All data [O1W distances from O22, or O23 carboxylato oxygen atoms, the water molecule atoms distances from Cu(COO)<sub>2</sub> plane, etc.] given in Table 2 together with the above discussed role of COO groups are in good agreement with the suggested ideas.<sup>[15,16]</sup>

**Table 3.** Dihedral angles /° of defined planes for **1–5**.

	P1–P2 ang <sup>a)</sup>	P1–P3 ang <sup>a)</sup>	(P1–Pi) <sub>aver</sub>	P2–P3 ang <sup>a)</sup>	$-2J / \text{cm}^{-1}$
<b>1</b>	5.16	0.76	2.96	5.87	8.15
<b>2</b>	8.49	13.64	11.06	7.43	6.57
<b>3</b>	2.35	3.29	2.82	0.94	8.57
<b>4</b>	4.25	9.02	6.64	4.25	6.82
<b>5</b>	3.62	8.36	5.99	4.74	6.45

a) P1 = the best plane defined by O12, Cu, O13, and O1 atoms; P2 = the best plane defined by O12, C02 and O22 atoms; P3 = the best plane defined by O13, C03 and O23 atoms.

The other parameters introduced in magnetic susceptibility evaluation, the  $zJ$  values, are of small and similar values due to similar chain structure of polymeric molecules (the same bridging denia ligands within the chains, the very similar Cu<sup>A</sup>–Cu<sup>B</sup>, or Cu<sup>A</sup>–Cu<sup>C</sup> distances, similar  $\pi$ – $\pi$ -stacking interactions of neighboring anion phenyl rings<sup>[17]</sup> (see Table 2). The denia ligand is no good mediator of magnetic interactions. Similar conclusions were drawn by magnetic analyses of some chain-like polymeric copper(II) complexes containing 3-pyridylmethanol as bridging ligand. They exhibited only very weak ferromagnetic interactions [18] within the chain ( $J = +0.12 \text{ cm}^{-1}$ ) and the obtained  $zJ = -0.07 \text{ cm}^{-1}$  value has been attributed to interchain interactions.

#### Spectral Properties of $[\text{Cu}(X\text{-sal})_2(\mu\text{-denia})(\text{H}_2\text{O})]_n$ (1–5)

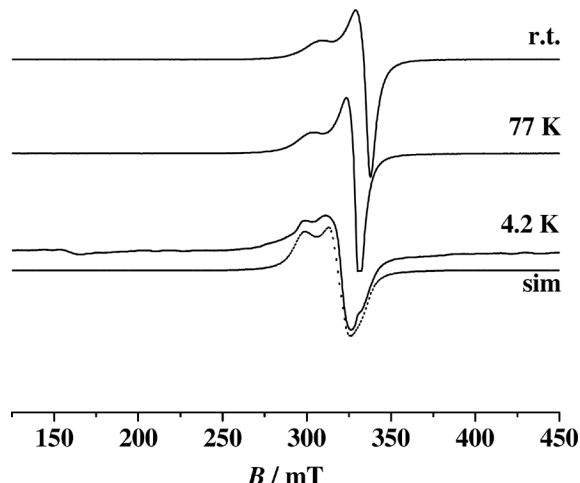
The EPR powder spectra of the presented complexes at room temperature are very similar and exhibit mostly the monomeric pattern of an axial symmetry except the spectrum of **2** (Figure S11) that shows only a single resonance attributed to isotropic signal (Table 4). The values of the  $g$  tensors  $g_{\parallel} > g_{\perp} > g_e$  are in good agreement with the observed square pyramidal structure with a  $d_{x^2-y^2}$  ground state.<sup>[19]</sup> Unresolved hyperfine splitting is observed as a consequence of strong dipolar and exchange interactions of the stacked molecules in solid state, which are in agreement with observed strong hydrogen bonds in studied complexes.

**Table 4.** The  $g$  tensor parameters obtained by simulation<sup>[20]</sup> spectra for compounds **1–5**.

	Temperature	$g_{\perp}$	$g_{\parallel}$
<b>1</b>	77 K	2.070	2.254
	room temp.	2.070	2.251
<b>2</b>	77 K	$g_i = 2.108$	
	room temp.	$g_i = 2.108$	
<b>3</b>	77 K	2.071	2.289
	room temp.	2.069	2.291
<b>4</b>	4.2 K	$g_x = 2.007$	$g_y = 2.067$
	77 K	2.080	2.270
	room temp.	2.078	2.274
<b>5</b>	4.2 K	2.068	2.231
	77 K	2.080	2.240
	room temp.	2.079	2.245

All EPR spectra in this study were also recorded at a temperature of 77 K, for complexes **3** and **4** spectra were obtained at 4.2 K.

Although most spectra show only small variations with decreasing temperature, some differences in the behavior of particular complexes were observed. The most interesting change with lowering of the temperature was found for **4**. The liquid helium temperature spectrum of **4** showed, in addition to splitting at about 335 mT, the presence of a clearly resolved half-field transition (159.6 mT), which was not seen in the spectrum at room temperature or at 77 K (Figure 5). This is in agreement with the triplet spin state with non-negligible zero-field splitting,<sup>[10]</sup> below 6 K and confirms a dimeric type of antiferromagnetic interactions.

**Figure 5.** EPR spectrum of **4** at room temperature, 77 K, and 4.2 K paired with the simulation.

The spectrum of complex **5** (Figure S13) at 77 K is similar to the room temperature spectrum. However, broadening of the perpendicular as well as of the parallel component is observed at liquid helium temperature. The spectra of **1** (Figure S10) and **3** (Figure S12) at room temperature and at 77 K are similar. For all obtained spectra, lowering of the temperature led to an increase of the signal line width as a consequence of strong dipolar and exchange interactions.<sup>[21]</sup>

The IR spectra of all complexes contain the bands corresponding to  $\nu_{as}(\text{COO}^-)$  and  $\nu_s(\text{COO}^-)$  at about  $1618 \text{ cm}^{-1}$  and  $1427 \text{ cm}^{-1}$ , respectively. The differences between antisymmetric and symmetric stretching ( $\Delta\nu = \nu_{as} - \nu_s$ ) are greater than  $\Delta\nu$  for the ionic form,<sup>[22]</sup> which is in agreement with the unidentate bonding mode of the carboxylate group proved by X-ray analysis (Table 5).

**Table 5.** The infrared spectra for compounds 1–5.

	$\nu_{\text{as}}(\text{COO}^-)$	$\nu_{\text{as}}(\text{COO}^-)$	$\Delta\nu^{\text{a})}$	$\Delta\nu_{\text{ion}}^{\text{b})}$
1	1620	1425	195	147
2	1619	1427	192	147
3	1615	1430	185	— <sup>c)</sup>
4	1636	1446	190	— <sup>c)</sup>
5	1630	1440	190	— <sup>c)</sup>

a)  $\Delta\nu = \nu_{\text{as}}(\text{COO}^-) - \nu_{\text{as}}(\text{COO}^-)$ . b)  $\Delta\nu_{\text{ion}}$  = for ionic form. c) Not known.

For all complexes broad bands of medium intensity and similar shape, which were attributed to O–H vibrations, are observed in the region of  $3200 \text{ cm}^{-1}$ – $3000 \text{ cm}^{-1}$ .

The solid state electronic spectra of the discussed complexes exhibit a broad asymmetric ligand field band with a maximum in the range of 638–632 nm. These d  $\leftarrow$  d spectra are typical for the square-pyramidal coordination polyhedra.<sup>[23]</sup> In addition, strong intraligand charge-transfer bands (250–300 nm) and LMCT bands (300–350 nm) were observed.

## Conclusions

Five coordination polymers formed by copper(II) salicylate with diethylnicotinamide were prepared and characterized. The crystal structures consist of 1D spiral-like polymeric chains that are held together by strong hydrogen bonds between coordinated water molecules of one chain and carboxylato groups of the neighboring chain, thus connected into 2D sheets. The supramolecular structure based on hydrogen O–H...O bonds [described by supramolecular synthons  $R_2^2(10)$  and  $R_2^2(12)$ ] is the pathway that causes antiferromagnetic interactions of the magnetically coupled pairs of copper atoms. The analyzed data allowed the suggestion that COO groups and coordinated water molecules are involved in dimeric magnetic interactions of the polymeric chain compounds. It should be underlined that the presented complexes are examples in which the structural dimensionality is different from the magnetic dimensionality. The careful analysis of the packing diagram is a very important step in understanding the magnetic behavior of polynuclear complexes, and in identifying the possible intermolecular exchange pathways.

## Experimental Section

### Physical Measurements

Carbon, hydrogen, and nitrogen analyses were carried out with a CHNSO FlashEA 1112 Automatic Elemental Analyzer. The copper content was determined by electrolysis of water solution obtained by the sample mineralization with a mixture of sulfuric acid and potassium peroxodisulfate.

The electronic spectra (190–1100 nm) of the complexes were measured in nujol suspension with a SPECORD 200 (Carl Zeiss Jena) spectrophotometer at room temperature. The infrared spectra (4000–1000  $\text{cm}^{-1}$ ) were recorded with a MAGNA 750 IR (Nicolet) and Nicolet 5700 FT-IR spectrophotometers at room temperature. EPR spectra of

the powdered samples were recorded with a spectrometer Bruker ER 200-SRC operating at X-band.

Magnetization measurements in the temperature range of 1.8–300 K were carried out on powdered samples of complexes, at the magnetic field 0.5 T, using a Quantum Design SQUID Magnetometer (type MPMS-XL5). Corrections for diamagnetism of the constituting atoms were calculated with Pascal's constants,<sup>[12]</sup> the value of  $60 \times 10^{-6} \text{ cm}^3 \cdot \text{mol}^{-1}$  was used as the temperature-independent paramagnetism of copper(II) ion. The best exchange parameters were obtained by fitting with a good agreement factor  $R$  defined:

$$R = \sum_{i=1}^n \frac{(\chi_i^{\text{exp}} T - \chi_i^{\text{calc}} T)^2}{(\chi_i^{\text{exp}} T)^2}$$

### Preparation of the Complexes

The blue complexes were prepared by similar reactions of aqueous solutions of copper(II) acetate with *N,N*-diethylnicotinamide and with appropriate salicylic acid with some addition of solvent (water or methanol as follows).

**[Cu(5-Mesal)<sub>2</sub>( $\mu$ -denia)(H<sub>2</sub>O)]<sub>n</sub>** (1) and **[Cu(3-Mesal)<sub>2</sub>( $\mu$ -denia)(H<sub>2</sub>O)]<sub>n</sub>** (2): *N,N*-diethylnicotinamide (0.17 mL, 1 mmol) was added to aqueous solution of copper(II) acetate (10 mL, 1 mmol) whilst stirring. After several minutes solid 5-, or 3-methylsalicylic acid (0.30 g, 2 mmol) and water (20 mL) were added to the solution. The reaction mixture was stirred for two days at ambient temperature. The blue precipitate was filtered off and the mother liquid was left to crystallize at room temperature. The formed crystals were separated and dried at ambient temperature. The composition of the powder products were according the elemental analyses and spectral characterizations the same as the crystal ones (proved by X-ray structure analysis).

**[Cu(4-MeOsal)<sub>2</sub>( $\mu$ -denia)(H<sub>2</sub>O)]<sub>n</sub>** (3): The initial procedure was the same as above with the exception that after several minutes solid 4-methoxysalicylic acid (0.33 g, 2 mmol) and water (190 mL) were added to the solution. The product isolation procedure was similar to the one described above.

**[Cu(3,5-Cl<sub>2</sub>sal)<sub>2</sub>( $\mu$ -denia)(H<sub>2</sub>O)]<sub>n</sub>** (4) and **[Cu(3,5-Br<sub>2</sub>sal)<sub>2</sub>( $\mu$ -denia)(H<sub>2</sub>O)]<sub>n</sub>** (5): The methanol solution (20 mL) of 3,5-dichlorosalicylic acid (0.15 g, 0.76 mmol) or 3,5-dibromosalicylic acid (0.22 g, 0.76 mmol) and *N,N*-diethylnicotinamide (0.13 mL, 0.77 mmol) was added to an aqueous solution of copper(II) acetate (20 mL, 0.32 mmol) whilst stirring. The formed precipitates were dissolved by addition of methanol (20 mL). The solutions were left for crystallization at ambient temperature. Formed crystals were separated and dried at ambient temperature. The compositions of the products were checked by elemental analyses and were proved by X-ray structure analyses.

**Analysis** **[Cu(5-Mesal)<sub>2</sub>( $\mu$ -denia)(H<sub>2</sub>O)]<sub>n</sub>** (1): C<sub>26</sub>H<sub>30</sub>CuN<sub>2</sub>O<sub>8</sub>: calcd. C 55.56; H 5.38; N 4.98; Cu 11.31 %; found: C 55.55; H 5.06; N 4.99; Cu 11.50 %.

**Analysis** **[Cu(3-Mesal)<sub>2</sub>( $\mu$ -denia)(H<sub>2</sub>O)]<sub>n</sub>** (2): C<sub>26</sub>H<sub>30</sub>CuN<sub>2</sub>O<sub>8</sub>: calcd. C 55.56; H 5.38; N 4.98; Cu 11.31 %; found: C 54.91; H 5.29; N 5.33; Cu 11.72 %.

**Analysis** **[Cu(4-MeOsal)<sub>2</sub>( $\mu$ -denia)(H<sub>2</sub>O)]<sub>n</sub>** (3): C<sub>26</sub>H<sub>30</sub>CuN<sub>2</sub>O<sub>10</sub>: calcd. C 52.57; H 5.09; N 4.72; Cu 11.31 %; found: C 51.44; H 5.09; N 5.10; Cu 11.50 %.

**Table 6.** Crystallographic data for compounds **1–5**.

	<b>1</b>	<b>2</b>	<b>3</b>	<b>4</b>	<b>5</b>
Code	ZP158/wal250	ZP91/ZP288	ZP171/wal7/ZV138TM	LM431/tg62	LM413/tg61
Chemical formula	C <sub>26</sub> H <sub>30</sub> CuN <sub>2</sub> O <sub>8</sub>	C <sub>26</sub> H <sub>30</sub> CuN <sub>2</sub> O <sub>8</sub>	C <sub>26</sub> H <sub>30</sub> CuN <sub>2</sub> O <sub>10</sub>	C <sub>24</sub> H <sub>22</sub> Cl <sub>4</sub> CuN <sub>2</sub> O <sub>8</sub>	C <sub>24</sub> H <sub>22</sub> Br <sub>4</sub> CuN <sub>2</sub> O <sub>8</sub>
M <sub>r</sub>	562.06	562.06	594.06	671.79	849.62
Cell setting, space group	Monoclinic, P2 <sub>1</sub> /n	Monoclinic, P2 <sub>1</sub> /n	Monoclinic, P2 <sub>1</sub> /n	Monoclinic, P2 <sub>1</sub> /n	Monoclinic, P2 <sub>1</sub> /n
Temperature /K	250(2) <sup>a</sup>	150(2)	100(2)	100(2)	100(2)
a /Å	16.598(5)	13.655(3)	14.297(5)	15.708(3)	15.861(1)
b /Å	8.126(3)	8.165(2)	8.155(3)	8.065(2)	8.105(1)
c /Å	19.980(6)	23.753(5)	22.388(9)	22.541(3)	22.955(2)
β /°	100.99(3)	104.74(3)	100.37(3)	105.86(1)	107.77(1)
V /Å <sup>3</sup>	2645.4(15)	2561.2(9)	2567.6(11)	2747.1(9)	2810.0(9)
Z	4	4	4	4	4
Radiation type	Mo-K <sub>α</sub>	Mo-K <sub>α</sub>	Mo-K <sub>α</sub>	Mo-K <sub>α</sub>	Mo-K <sub>α</sub>
μ /mm <sup>-1</sup>	0.88	0.91	0.91	1.24	6.52
Crystal size /mm	0.35 × 0.18 × 0.10	0.36 × 0.19 × 0.07	0.30 × 0.20 × 0.09	0.40 × 0.30 × 0.25	0.40 × 0.35 × 0.26
No. of reflections, No. of parameters	5356, 327	5099, 340	5227, 368	4705, 368	4858, 368
R <sub>int</sub>	0.061	0.056	0.061	0.066	0.120
R [F <sup>2</sup> > 2σ(F <sup>2</sup> )],	0.050, 0.102, 1.06	0.039, 0.078, 1.04	0.044, 0.080, 1.065	0.050, 0.124, 1.10	0.055, 0.107, 1.11
wR(F <sup>2</sup> ), S					
Δρ <sub>max</sub> , Δρ <sub>min</sub> / e·Å <sup>-3</sup>	0.27, -0.27	0.27, -0.31	0.37, -0.30	0.52, -0.60	0.64, -0.70

a) X-ray data of complex **1** were firstly obtained at 100 K but they were not suitable for solving structure.<sup>[30]</sup>

**Analysis** [Cu(3,5-Cl<sub>2</sub>sal)<sub>2</sub>(μ-denia)(H<sub>2</sub>O)]<sub>n</sub> (**4**): C<sub>26</sub>H<sub>26</sub>Cl<sub>4</sub>CuN<sub>2</sub>O<sub>8</sub>: calcd. C 42.91; H 3.30; N 4.17; Cu 9.46 %; found: C 42.45; H 3.16; N 3.99; Cu 10.03 %.

**Analysis** [Cu(3,5-Br<sub>2</sub>sal)<sub>2</sub>(μ-denia)(H<sub>2</sub>O)]<sub>n</sub> (**5**): C<sub>26</sub>H<sub>26</sub>Br<sub>4</sub>CuN<sub>2</sub>O<sub>8</sub>: calcd. C 33.93; H 2.61; N 3.29; Cu 7.48 %; found: C 34.15; H 2.06; N 3.49; Cu 7.50 %.

### X-ray Crystallography

The crystal data and details of data collections for all structures are given in Table 6. Intensity data were collected with a diffractometer Kuma KM-4 CCD<sup>[24]</sup> or a Bruker-Nonius KappaCCD<sup>[25]</sup> with graphite monochromated Mo-K<sub>α</sub> radiation. The diffraction intensities were corrected for Lorentz and polarization effects. Absorption corrections were applied using the programs CrysAlis-RED<sup>[24]</sup> or SADABS.<sup>[26]</sup> The structures were solved by direct methods using the programs SHELXS-97<sup>[27]</sup> or SIR-97<sup>[28]</sup> and refined by the full-matrix least-squares method on all F<sup>2</sup> data using the program SHELXL-97.<sup>[27]</sup> Geometrical analyses were performed using SHELXL-97 program. The structures were drawn by XP in SHELXTL<sup>[27]</sup> and MERCURY<sup>[29]</sup> programs.

The one of the 5-methylsalicylate ligands as well as the one of the methyl group of *N,N*-diethylnicotinamide ligands of complex **1** are disordered and the refined site-occupancy factors of the two disordered parts are 0.42 and 0.58, respectively, for both disordered groups. The C–C, C–O, C···C, and C···O distances were restrained by SADI instructions of SHELXL-97. Thermal ellipsoids of disordered nitro groups were constrained by EADP instructions of SHELXL-97.

The hydroxyl group of one of the 4-methoxysalicylate ligands of **3** is disordered and the refined site-occupancy factors of the two disordered parts are 0.48 and 0.52, respectively. Thermal ellipsoids of disordered nitro-groups have been constrained by EADP instructions.

The both hydroxyl group of both of the 3,5-dichlorosalicylate ligands of **4** are disordered and the refined site-occupancy factors of the two disordered parts are 0.70 and 0.10; 0.91, and 0.09. One of the ethyl groups of *N,N*-diethylnicotinamide ligand of **4** is disordered and the refined site-occupancy factors of the two disordered parts are 0.43 and 0.57, respectively. Similarly, both hydroxyl groups of the 3,5-dibromo-salicylate ligands of **5** are disordered and the refined site-occupancy factors of the two disordered parts are 0.73 and 0.27; 0.88, and 0.12, respectively. One of the ethyl groups of *N,N*-diethylnicotinamide ligand of **5** is disordered and the refined site-occupancy factors of the two disordered parts are 0.42 and 0.58, respectively. Thermal ellipsoids of disordered nitro groups were constrained by EADP instructions. The C–C and C···C distances were restrained by SADI instructions. Thermal ellipsoids of disordered nitro-groups were constrained by EADP instructions.

Crystallographic data for the structural analysis have been deposited with the Cambridge Crystallographic Data Centre CCDC nos. CCDC-774006 (**1**), -774007 (**2**), -774008 (**3**), -774009 (**4**), and CCDC-774010 (**5**). Further details of the crystal structures investigations are available free of charge via [www.ccdc.cam.ac.uk/conts/retrieving.html](http://www.ccdc.cam.ac.uk/conts/retrieving.html) (or from the CCDC, 12 Union Road, Cambridge CB2 1EZ, UK; Fax: +44-1223-336033; E-Mail: deposit@ccdc.cam.ac.uk).

**Supporting Information** (see footnote on the first page of this article): The supplementary Figures S1–S13 and Table S1.

### Acknowledgement

This work was supported by the *Slovak Research and Development Agency* under the contract No. VVCE-0004-07. We thank *Ministry of Education of the Czech Republic* (Project VZ0021627501), and *University of Wroclaw* for financial support.

## References

- [1] a) A. M. Beatty, *Coord. Chem. Rev.* **2003**, *246*, 131–143; b) P. Hubberstey, U. Suksangpanya, *Struct. Bonding* **2004**, *111*, 33–83.
- [2] A. D. Burrows, C. W. Chan, M. M. Chowdhry, J. E. McGrady, D. M. P. Mingos, *Chem. Soc. Rev.* **1995**, *24*, 329–339.
- [3] a) D. Braga, F. Grepioni, G. R. Desiraju, *Chem. Rev.* **1998**, *75*, 1375–1405; b) A. D. Burrows, *Struct. Bonding* **2004**, *108*, 55–96.
- [4] J.-Y. Lee, O. K. Farha, J. Roberts, K. A. Scheidt, S. T. Nquyen, J. T. Hupp, *Chem. Soc. Rev.* **2009**, *38*, 1450–1459.
- [5] M. D. Allendorf, C. A. Bauer, R. K. Bhakta, R. J. T. Houk, *Chem. Soc. Rev.* **2009**, *38*, 1330–1352.
- [6] a) M. Kurmoo, *Chem. Soc. Rev.* **2009**, *38*, 1353–1379; b) J. M. Moreno, J. Ruiz, J. M. Dominguez-Vera, E. Colacio, *Inorg. Chim. Acta* **1993**, *208*, 111–115; c) W. Plass, A. Pohlmann, J. Rautengarten, *Angew. Chem. Int. Ed.* **2001**, *40*, 4207–4210.
- [7] O. R. Evans, W. B. Lin, *Acc. Chem. Res.* **2002**, *35*, 511–522.
- [8] J.-R. Li, R. J. Kuppler, H.-C. Zhou, *Chem. Soc. Rev.* **2009**, *38*, 1477–1504.
- [9] D. Valigura, J. Moncol, M. Korabik, Z. Púčeková, T. Lis, J. Mrožínski, M. Melník, *Eur. J. Inorg. Chem.* **2006**, 3813–3817.
- [10] Z. Vasková, J. Moncol, M. Korabik, D. Valigura, J. Švorec, T. Lis, M. Valko, M. Melník, *Polyhedron* **2010**, *29*, 154–164.
- [11] B. Bleaney, K. D. Bowers, *Proc. R. Soc. A* **1952**, *214*, 451–464.
- [12] O. Kahn, *Molecular Magnetism*, VCH Publishers, New York, 1993.
- [13] T. Kawata, H. Uekusa, S. Ohba, T. Furukawa, T. Tokii, Y. Muto, M. Kato, *Acta Crystallogr., Sect. B* **1992**, *48*, 253–261.
- [14] J. Tang, J. S. Costa, A. Golobič, B. Kozlevčar, A. Robertazzi, A. V. Vargiu, P. Gamez, J. Reedijk, *Inorg. Chem.* **2009**, *48*, 5473–5479.
- [15] Y. Yamada, N. Ueyama, T. Okamura, W. Mori, A. Nakamura, *Inorg. Chim. Acta* **1998**, *275*–276, 43–51.
- [16] C. Desplanches, E. Ruiz, A. Rodríguez-Fortea, S. Alvarez, *J. Am. Chem. Soc.* **2002**, *124*, 5197–5205.
- [17] C. Janiak, *Dalton Trans.* **2003**, 2781–2804.
- [18] P. Stachová, M. Korabik, M. Koman, M. Melník, J. Mrozinksi, T. Glowiaik, M. Mazúr, D. Valigura, *Inorg. Chim. Acta* **2006**, *359*, 1275–1281.
- [19] a) B. J. Hathaway, A. A. G. Tomlinson, *Coord. Chem. Rev.* **1970**, *5*, 1–43; b) B. J. Hathaway, D. E. Billing, *Coord. Chem. Rev.* **1970**, *5*, 143–207.
- [20] a) H. Thiele, J. Etstling, P. Such, P. Hoefer, *WIN-EPR*, Bruker Analytik GmbH, Bremen and Rheinstetten, Germany, **1992**; b) R. T. Weber, *WIN-EPR SimFonia*, Software version 1.2, EPR Division, Bruker Instruments, Inc., Billerica, USA, **1995**.
- [21] C. Karunakaran, K. R. Justin Thomas, A. Shumugusundaran, R. Murugesan, *Mol. Phys.* **2002**, *100*, 287–295.
- [22] a) K. Nakamoto, *Infrared and Raman Spectra of Inorganic and Coordination Compounds*, Wiley-Interscience, New York, **1997**; b) G. B. Deacon, R. J. Phillips, *Coord. Chem. Rev.* **1980**, *33*, 227–250.
- [23] A. B. P. Lever, *Inorganic Electronic Spectroscopy*, Elsevier, Amsterdam **1984**.
- [24] Oxford Diffraction, *CrysAlis CCD* and *CrysAlis RED*, Oxford Diffraction Ltd, Abingdon, England, 2006.
- [25] a) R. W. Hooft, *COLLECT*, Nonius BV, Delft, The Netherlands, **1998**; b) A. J. M. Duisenberg, L. M. J. Kroon-Batenburg, A. M. M. Schreurs, *J. Appl. Crystallogr.* **2003**, *36*, 220–229.
- [26] G. M. Sheldrick, *SADABS*, Bruker AXS Inc., Madison, Wisconsin, USA, 2003.
- [27] A. Altomare, M. C. Burla, M. Camalli, G. L. Cascarano, C. Giacovazzo, A. Guagliardi, A. G. G. Moliterni, G. Polidori, R. Spagna, *J. Appl. Crystallogr.* **1999**, *32*, 115–119.
- [28] G. M. Sheldrick, *Acta Crystallogr., Sect. A* **2008**, *64*, 112–122.
- [29] C. F. Macrae, P. R. Edgington, P. McCabe, F. Pidcock, G. P. Shields, R. Taylor, M. Towler, J. van de Streek, *J. Appl. Crystallogr.* **2006**, *39*, 453–457.
- [30] DSC measurements of complex **1** has been done and it confirmed that almost reversible phase change at about 200 K (Figures S8 and S9) proceeds. Then the temperature for X-ray structure determination was set to be 250 K. The later analysis of data obtained at 100 K [ $a = 16.281(5)$ ,  $b = 8.065(3)$ ,  $c = 19.960(6)$  Å,  $\beta = 99.500(3)^\circ$ ,  $V = 2584.9(15)$  Å<sup>3</sup>,  $Z = 4$ ,  $T = 100(2)$  K, Monoclinic, Space group  $P2_1/n$ , CCDC no. CCDC-795186] and its comparison with dataset for 250 K has indicated that the phase transition is not connected with the crystal structure and symmetry changes.

Received: July 30, 2010

Published Online: December 29, 2010